

Thermal birefringence and depolarization compensation in glass-based high-average-power laser systems

Amber L. Bullington*, Steven B. Sutton, Andy J. Bayramian, John A. Caird, Robert J. Deri, Al C. Erlandson, Mark A. Henesian

Lawrence Livermore National Laboratory, 7000 East Avenue, Livermore, CA, USA 94550

ABSTRACT

Thermally induced birefringence can degrade the beam quality in high-average-power laser systems with doped-glass substrates. In this work, we compare glass-laser slab amplifiers at either Brewster's angle or normal incidence and discuss trade-offs between both designs. Numerical simulations show the impact of thermally induced depolarization in both amplifier systems. A non-uniform temperature profile and the resultant mechanical stress leads to depolarization that worsens as the beam propagates through the slab-amplifier chain. Reflective losses for depolarized light at Brewster's angle cannot be compensated and degrade beam quality. This motivates the selection of normally incident slab amplifiers, which facilitates birefringence compensation.

Tolerances for birefringence compensation of two matched normal-incidence glass-slab amplifiers balanced by a quartz rotator are also investigated. Imbalances in thermal load, relative amplifier position and beam magnification between amplifiers show the highest depolarization sensitivity and establish limits for manufacturing tolerances and amplifier design.

Keywords: thermal birefringence, depolarization, high-average-power lasers

1. INTRODUCTION

Thermally induced stress birefringence can present challenges for high-average-power lasers, including those with glass as the host material. Non-uniform heating of a glass slab creates thermal gradients at the pump-beam edges resulting in stress birefringence that depolarizes the beam. Excessive birefringence can have negative effects on beam quality, especially when polarized output is required.

Laser amplifiers with glass slabs positioned at either Brewster's angle or normal incidence are both susceptible to thermal birefringence. P-polarized reflectivity is zero at Brewster's angle, providing the advantage of not requiring anti-reflective (AR) coatings that may damage under high-power operation. However, any light depolarized in a Brewster's angle slab amplifier experiences a high reflective loss. In this work, we investigate thermally induced depolarization in Brewster's angle slabs to determine beam quality degradation and compare the results to slabs at normal incidence. The results motivate the use of AR-coated normal incidence slabs with birefringence compensation.

A balanced-amplifier compensation scheme is also presented. Two amplifiers, equally pumped with the same number of slabs, are birefringence-compensated via a polarization rotator. Imbalances in the amplifiers giving the highest residual depolarization are discussed. These potential asymmetries determine the tightest tolerances for amplifier design.

*bullington1@llnl.gov; phone 925-423-7589; fax 925-423-6195

2. ANALYZING THERMAL BIREFRINGENCE

Thermal birefringence is modeled using a multi-step method that links data from finite-element analysis to a ray-tracing program for analyzing beam depolarization. Finite-element modeling of the temperature profile and stress are performed for a given heat deposition profile. These results serve as inputs to a ray-tracing program that calculates the Jones matrices for determining the beam depolarization as a function of position for a single slab. An additional script multiplies these Jones matrices to determine the beam depolarization in a multi-slab amplifier. A flowchart of the analysis is given in Figure 1. The finite-element thermal and stress analyses as well as the depolarization ray-trace model are based on validated codes that have been tested and previously published in the literature [1]. Multiplying Jones matrices for multiple-slab amplifiers is performed with a MATLAB script.

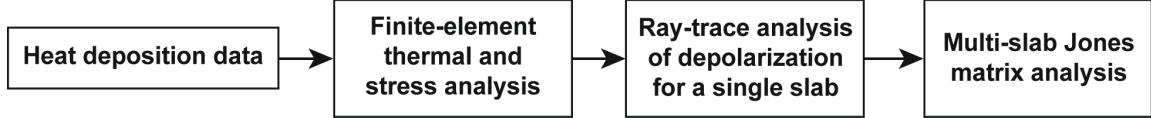


Figure 1. A flowchart summarizes the numerical analysis of the thermal birefringence.

The heat deposition is given by an analytical super-Gaussian pump profile of order n and half-width w that can be written as

$$SG(x, y) = \exp\left[-(x^n + y^n)/w^n\right]. \quad (1)$$

The depolarization ray-trace analysis treats each finite element composing the slab as a linear retarder. At each element, rays are traced through the thickness of the slab to determine the Jones matrix for each spatial coordinate. The Jones matrix for given x and y coordinates on a single slab can be written as

$$R(\psi, \delta) = \begin{bmatrix} \cos[\delta(x, y)/2] & 0 \\ 0 & \cos[\delta(x, y)/2] \end{bmatrix} + i \begin{bmatrix} -\cos[2\psi(x, y)]\sin[\delta(x, y)/2] & -\sin[2\psi(x, y)]\sin[\delta(x, y)/2] \\ -\sin[2\psi(x, y)]\sin[\delta(x, y)/2] & \cos[2\psi(x, y)]\sin[\delta(x, y)/2] \end{bmatrix} \quad (2)$$

where

$$\delta(x, y) = \frac{2\pi l}{\lambda} (n_x - n_y) \quad (3)$$

is the retardation and $\psi(x, y)$ is the rotation angle of the retarder axis [2-4]. l is the distance traversed through the medium and n_x and n_y are the refractive indices along the axes in the coordinate frame of the slab element being ray-traced. The depolarization for a multi-slab amplifier is calculated from the product of the Jones matrices comprising the individual slabs. For an amplifier with n identical slabs, it can be shown that the amplifier's Jones matrix is equal to

$$R(\psi, \delta)^n = \begin{bmatrix} \cos[n\delta(x, y)/2] & 0 \\ 0 & \cos[n\delta(x, y)/2] \end{bmatrix} + i \begin{bmatrix} -\cos[2\psi(x, y)]\sin[n\delta(x, y)/2] & -\sin[2\psi(x, y)]\sin[n\delta(x, y)/2] \\ -\sin[2\psi(x, y)]\sin[n\delta(x, y)/2] & \cos[2\psi(x, y)]\sin[n\delta(x, y)/2] \end{bmatrix}, \quad (4)$$

where the retardation is multiplied by the number of slabs, n . The depolarization for a multi-slab amplifier is given by [2,3]

$$Depol = \sin[2\psi(x, y)]^2 \sin[n\delta(x, y)/2]^2. \quad (5)$$

For analyses in this paper, the incident light is assumed to be p-polarized. The depolarization is given by the power converted to s-polarization. When circularly polarized light is propagated through an amplifier system, the output field is multiplied by an analytical quarter-wave plate to convert to linear polarization.

3. AMPLIFIER WITH BREWSTER'S ANGLE SLABS

Amplifiers constructed with Brewster's angle slabs have the advantage of not requiring AR coatings. While p-polarized light experiences no reflective loss at Brewster's angle, s-polarized light has a 16% reflective loss at each slab interface. Any depolarized light sees a power loss from multiple reflective surfaces. The loss for a 44-slab amplifier is analyzed in this section.

3.1 Analysis with a theoretical super-Gaussian pump profile

Figure 2a shows the temperature distribution at the slab-center for a super-Gaussian pump beam of order $n = 20$ and half-width $w = 20$ cm incident on a 42 cm by 42 cm glass slab. The slab thickness is 1 cm. The pump beam is normally incident on the Brewster's angle slab. The front and back faces of the slab are cooled with flowing gas. Since the slabs are oriented at Brewster's angle, the transmitted beam is rectangular with dimensions 22 cm by 40 cm. The 40 cm by 40 cm inner window defines the extent of the ray-trace for depolarization analysis. Any roll-off of the transmitted beam is assumed to occur in the 2-cm border region of the slab. The temperature gradients from pump-beam roll-off lead to shear stress extending into the slab in Figure 2b. The maximum heat deposition is 1.66 W/cm^3 .

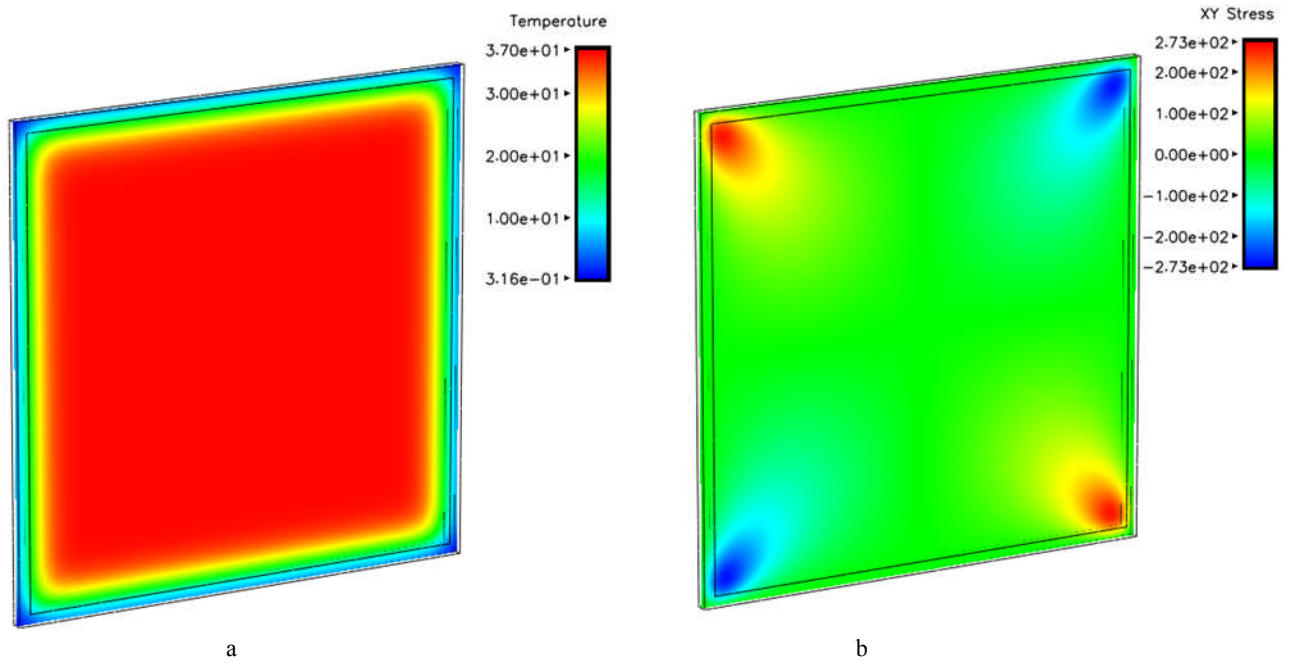


Figure 2. Plot (a) shows the temperature profile in degrees Celcius at the center of the slab with heat deposition data determined by a super-Gaussian pump profile. Plot (b) shows the resultant shear stress at slab-center in N/cm^2 . The slab dimensions are 42 cm by 42 cm. The inner window is 40 cm by 40 cm and defines the extent of the beam for ray-trace analysis.

The depolarization for a single Brewster's angle slab is shown in Figure 3 with a maximum depolarization of 54%. The x-dimension is shortened because of the Brewster's angle orientation of the slab.

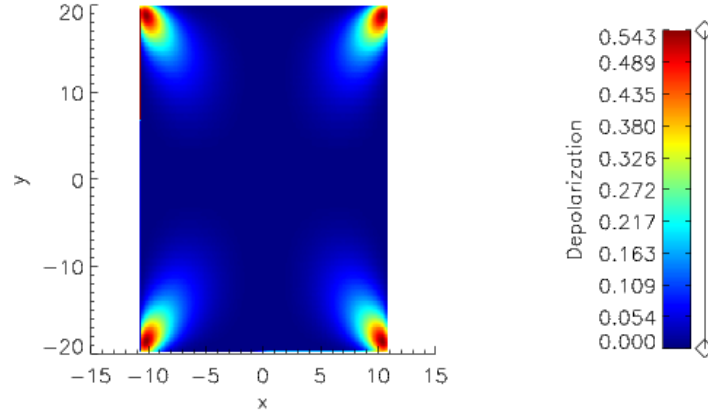


Figure 3. A map of depolarization is shown given the temperature and stress from Figure 2. The map in the x-dimension is reduced due to the Brewster's angle orientation of the slab.

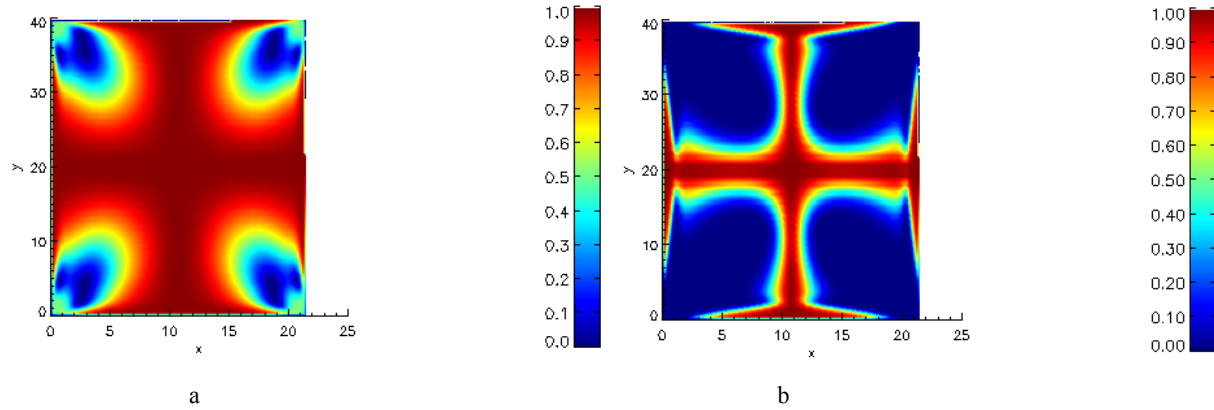


Figure 4. Image (a) shows the transmitted p-polarized light after traversing four Brewster's angle slabs. Image (b) shows the transmitted beam after double-passing a 44-slab amplifier (88 passes through Brewster's angle slabs). Both images use temperature and stress data from Figure 2 and include the 16% per interface reflective loss seen by the depolarized light. Gain is not included.

Figure 4 shows the p-polarized transmitted beam after traversing (a) four slabs and (b) a double-pass of an amplifier with 44 slabs. Gain is not included in the calculation. Figure 4b demonstrates that traversing multiple slabs compounds the depolarization loss. By double-passing a Brewster-slab amplifier that includes traversing 44 individual slabs twice and encountering 176 reflective interfaces, the depolarized light at the slab corners is lost. This creates a transmitted beam with an iron-cross shape instead of the desired flat-beam profile across the slab aperture. The fraction of power remaining in p- and s-polarization for single- and double-passing the amplifier is given in Table 1. Only 0.3% of the s-polarized light and 26% of the p-polarized light remains after a double pass. Lost power as a function of the number of slabs traversed during a double pass is shown in Figure 5. For a double-passing a 44-slab amplifier, the lost power reaches 75%. Transmitted-beam degradation must be overcome for Brewster's angle slabs to be a viable option for high-average-power laser systems.

Table 1. The fraction of average power in each polarization is given after a single- and double-pass of a 44-slab amplifier. 16% reflective loss for s-polarization at each interface is included.

	Single Pass	Double Pass
P-polarized light	0.3285	0.2600
S-polarized light	0.0080	0.0030

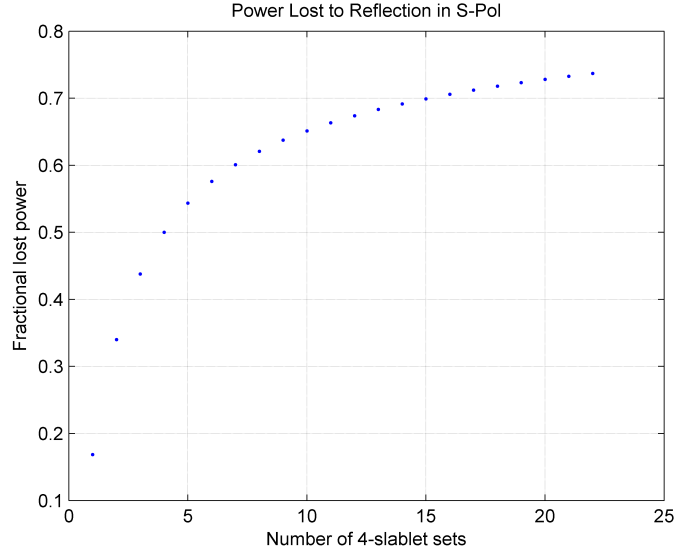


Figure 5. The fraction of power lost from reflected s-polarized light is shown as a function of the number of slabs traversed for a double-pass of the amplifier.

3.2 Varying the super-Gaussian pump profile

A uniform pump profile with a sharp roll-off at the edges may minimize depolarization from thermal birefringence. Super-Gaussian pump profiles of varying half-widths, w , and order, n , are tested with Brewster's angle slabs. The average depolarization for a 42 cm by 42 cm slab is shown in Table 2. Overfilling the pump beam on the slab reduces the magnitude of the temperature gradients from pump roll-off, thereby reducing the depolarization. Increasing the order of the super-Gaussian from $n = 20$ to $n = 30$ increases the rate of pump roll-off. However, Table 2 shows that overfilling the pump beam on the slab is more beneficial than increasing the pump roll-off.

Table 2. Individual slab depolarization is given for various super-Gaussian pump profiles on a 42 cm x 42 cm slab.

Super-Gaussian	Single-slab average depolarization	Pump-beam overfill loss
$w = 19$ cm, $n = 20$	0.1567	0.2%
$w = 19$ cm, $n = 30$	0.1517	0.01%
$w = 20$ cm, $n = 20$	0.0797	2.3%
$w = 21$ cm, $n = 20$	0.0244	7.4%
$w = 22$ cm, $n = 20$	0.0053	14%

From Table 2, a super-Gaussian half-width of 22 cm gives an average depolarization of 0.5% for a single Brewster's angle slab. However, the pump power lost from overfilling the super-Gaussian profile on the slab is 14%. The depolarized light lost to reflection when double-passing 44 slabs is 55% when $w = 22$ cm compared to 75% for $w = 20$ cm observed in Figure 5.

Reducing depolarization in a Brewster-slab amplifier involves sacrificing pump efficiency by overfilling the slab with pump light while still suffering high losses from reflected depolarized light. Losing pump efficiency to reduce depolarization does not provide sufficient benefit to improving performance of a Brewster's angle slab amplifier. As a result, normally incident slab amplifiers are considered over Brewster's angle slabs.

4. AMPLIFIER WITH NORMAL-INCIDENCE SLABS

Figure 6 shows the depolarization pattern, excluding reflective loss, for a normally incident slab pumped by a super-Gaussian beam of order 20 with a half-width of 11.5 cm. The incident beam is assumed to have the same dimensions as the pump beam. The slab dimensions are 26 cm by 26 cm with a heat load of 2.27 W/cm^3 . The slab thickness is 1 cm and the slab faces are gas-cooled. Figure 7 shows the maximum p-polarized transmission after a single pass through a 22-slab amplifier and includes 0.1% AR-coating reflective loss at each interface. The periodic variation seen in Figure 7 that resembles an isogyre pattern stems from the phase wrapping that occurs once the retardation (Eqn. 3) reaches 2π . Note that both p- and s-polarizations at normal incidence experience equal reflective loss as opposed to the Brewster's angle case. Thus, any depolarized light is still present with equal power compared to the power of the desired polarization in the system. Clearly, depolarization is a problem for normal-incidence slabs if polarized output is required. However, equal reflective loss for s- and p-polarized light allows for birefringence compensation.

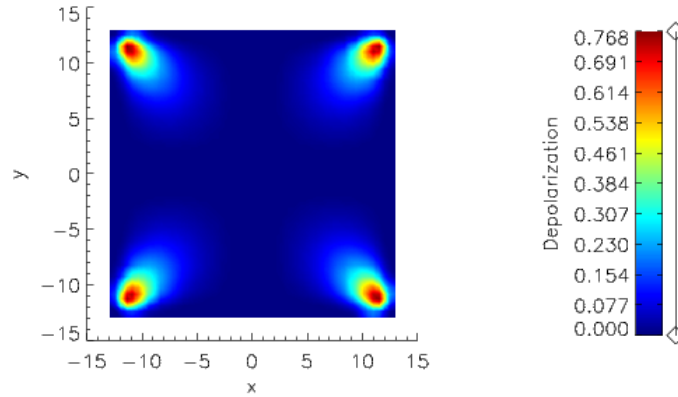


Figure 6. The depolarization for a normally incident slab is shown given a heat load of 2.27 W/cm^3 .

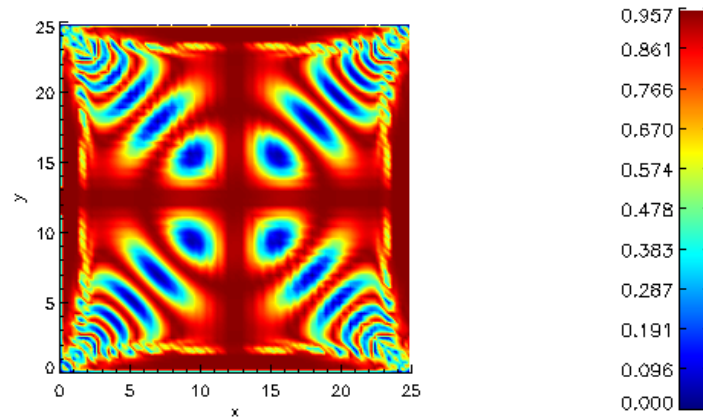


Figure 7. Maximum p-polarized transmission is shown after a single-pass of a 22-slab amplifier. An AR-coating loss of 0.1% is included at each interface and affects both p- and s-polarizations equally.

5. BIREFRINGENCE COMPENSATION

One method for compensating thermal birefringence involves placing a polarization rotator between two identical amplifiers [5,6]. Figure 8 shows a schematic of a balanced compensation scheme. A quartz rotator rotates the polarization by 90 degrees. This allows any depolarized light to experience an equal and opposite phase retardation in the second amplifier, thereby eliminating depolarization. The incident light is linearly polarized, while the light traversing the amplifiers is converted to circular polarization via a quarter-wave plate to reduce nonlinear focusing related to B-integral [7,8]. Depolarization is analyzed by converting output circular polarization to linear polarization with a Jones matrix for a quarter-wave plate and noting the residual depolarized light. The mirror in Figure 8 may be replaced with a quarter-wave plate for calculating single-pass depolarization to convert the circularly polarized light back to linear polarization.

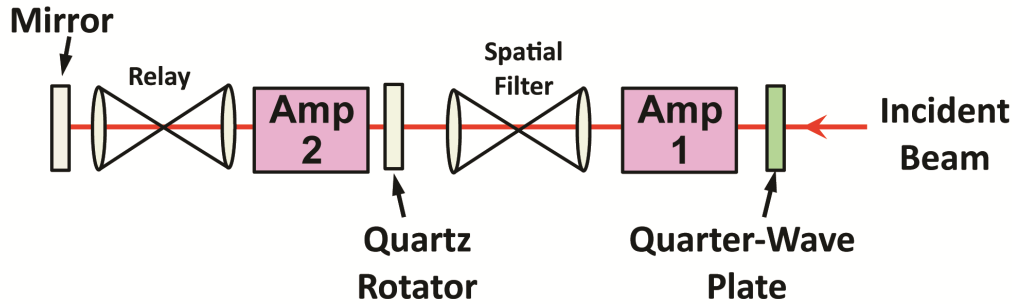


Figure 8. A birefringence compensation scheme using two balanced amplifiers (Amp) and a quartz rotator is shown with relay imaging optics and a spatial filter. A mirror is used to double-pass the amplifier, but may be exchanged for a quarter-wave plate for single-pass depolarization analysis. The incident light is linearly polarized but is converted to circular polarization with a quarter-wave plate.

Imbalances between amplifiers and residual depolarization are addressed in this section. Differences in amplifiers 1 and 2 that have the tightest tolerances are addressed, including a heat imbalance between amplifiers, one amplifier offset in position with respect to the other, and a beam magnification error in one amplifier. Thermal loading in the quartz rotator is also discussed.

5.1 Birefringence compensation with increased heat load in one amplifier

Table 3 lists the percentage of depolarized light remaining after compensation when amplifier 2 has a higher heat load than amplifier 1. Double-passing the system with only 2% higher heat in one amplifier leads to 5.4% residual depolarization. To keep any residual depolarization below a nominal value of 2%, the heat load in each amplifier must agree to within 1%.

Table 3. Depolarization after birefringence compensation with amplifier 2 running hotter than amplifier 1.

Heat Increase, Amplifier 2	Single-Pass Depolarization	Double-Pass Depolarization
1% Hotter	0.56%	1.56%
2% Hotter	2.1%	5.4%

5.2 Birefringence compensation with a position offset for one amplifier

If one amplifier is offset in position with respect to the other, significant depolarization can remain after compensation. Amplifier 2 is offset laterally with respect to amplifier 1 by varying amounts as listed in Table 4. An offset of only 1 mm gives a single-pass residual depolarization of 4%.

Table 4. Depolarization with one amplifier offset laterally in position with respect to the other.

Position Offset	Single-Pass Depolarization
200 μm	0.71%
400 μm	2.3%
600 μm	3.5%
800 μm	3.9%
1 mm	4.0%

Figure 9 shows the transmitted beam images for amplifier offsets of 200 μm and 1 mm. The beam distorts around the edges with increasing offset. AR-coating loss of 0.1% is included in the plots. Each amplifier must be positioned to less than 1 mm accuracy to keep lateral-offset depolarization to a minimum.

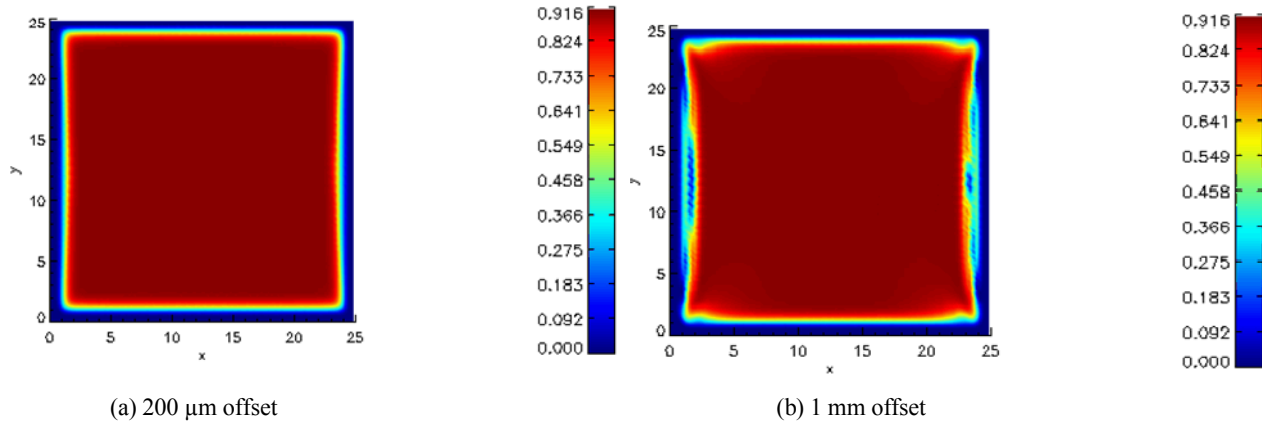


Figure 9. Transmitted beam images from a single pass of two compensated amplifiers with one amplifier offset to the right by (a) 200 μm and (b) 1 mm. An AR-coating loss of 0.1% is included.

5.3 Birefringence compensation with a magnification error

The beam must be reimaged from one amplifier into the other via a relay telescope. If the telescope does not relay the beam with perfect one-to-one imaging, the beam will sample a larger area of one amplifier compared to the other amplifier. Table 5 gives the residual depolarization as a function of increase in beam diameter. The depolarization increases rapidly with magnification error. This offers a guideline for determining manufacturing tolerances on the relay telescope elements.

Table 4. Depolarization from a relay telescope magnification error. The second amplifier experiences the given increase in beam diameter.

Beam Diameter Increase	Single-Pass Depolarization
200 μm	0.43%
400 μm	1.7%
600 μm	3.5%
1 mm	7.5%

5.4 Thermal loading of the quartz rotator

Thermal variation of rotation in quartz has been investigated by Chandrasekhar [9, 10]. At the operating wavelength of 1053 nm, the rotation per mm, ρ , has a temperature dependence, $d\rho/dT$, of 7.643×10^{-4} deg/mm/K. This equates to a variation in ρ of 0.11% for a 10 degree increase in temperature. Thus, temperature variation of polarization rotation in quartz at 1053 nm is quite small and should not pose a problem for birefringence compensation.

6. CONCLUSION

Depolarization losses that are overcome at the expense of efficiency make Brewster's angle slab amplifiers a less attractive option than normal-incidence slab amplifiers. Normally incident slab amplifiers allow for depolarization losses to be compensated with balanced amplifiers and a quartz rotator. By meeting the system design tolerances determined by residual depolarization discussed in section 5, the normally incident slab amplifier is a promising option for a high-average-power laser system.

This work was performed under the auspices of the U.S. Department of Energy by Lawrence Livermore National Laboratory under Contract DE-AC52-07NA27344.

REFERENCES

- [1] Rotter, M., Jancaitis, K., Marshall, C., Zapata, L., Erlandson, A., LeTouze, G., and Seznec, S., "Pump-induced wavefront distortion in prototypical NIF/LMJ amplifiers – modeling and comparison with experiments," Proc. SPIE 3492, 638-659 (1999).
- [2] Rotter, M., "An algorithm for depolarization," LLNL internal memo, (1998).
- [3] Chen, Y., Chen, B., Patel, M. K. R., and Bass, M., "Calculation of thermal-gradient-induced stress birefringence in slab lasers - I," IEEE J. Quant. Elec. 40(7), 909-916 (2004).
- [4] Giuliani, G. and Ristori, P., "Polarization flip cavities: a new approach to laser resonators," Opt. Comm. 35(1) 109-112 (1980).
- [5] Frede, M. Wilhelm, R., Brendel, M., Fallnich, C., Seifert, F., Willke, B., and Danzmann, K., "High power fundamental Mode Nd:YAG laser with efficient birefringence compensation," Opt. Express, 12(15) 3581-3589 (2004).
- [6] Frede, M. Wilhelm, R., Gau, R., Brendel, M., Zawischa, I., Fallnich, C., Seifert, F., and Willke, B., "High-power single-frequency Nd:YAG laser for gravitational wave detection," Classical and Quantum Gravity, 21, 895-901 (2004).
- [7] Feldman, A., Horowitz, D., and Waxler, R., "Mechanisms for self-focusing in optical glasses," IEEE J. Quantum Electron., QE-9, 1054-1061 (1973).
- [8] Auric, D., and Labadens, A. "On the use of a circularly polarized beam to reduce the self-focusing effect in a glass rod amplifier," Opt. Comm., 21, 241-242 (1977).
- [9] Chandrasekhar, S. "The Optical Rotary Power of Quartz and its Variation with Temperature," Proceedings of the Indian Academy of Sciences, 35, 103-113 (1951).
- [10] Chandrasekhar, S. "The Temperature Variation of the Rotary Power of Quartz from 30 deg to 410 deg C," Proceedings of the Indian Academy of Sciences, 39, 290-295 (1954).